https://doi.org/10.5194/acp-2020-574
Preprint. Discussion started: 8 July 2020

Atmospheric Chemistry and Physics Discussions

Black Carbon Seasonal and Diurnal Variation in surface snow in Svalbard and its Connections to Atmospheric Variables

Michele Bertò[1#], David Cappelletti[2,7], Elena Barbaro[1,3], Cristiano Varin[1], Jean-Charles Gallet[4], Krzysztof Markowicz[5], Anna Rozwadowska[6], Mauro Mazzola[7], Stefano Crocchianti[2], Luisa Poto[1,3], Paolo Laj[8], Carlo Barbante[1,3] and Andrea Spolaor[1,2].

[1]Ca' Foscari University of Venice, Dept. Environmental Sciences, Informatics and Statistics, via Torino, 155 - 30172 Venice-Mestre, Italy;
[2]Università degli Studi di Perugia, Dipartimento di Chimica, Biologia e Biotecnologie, Perugia, Italy;
[3]CNR-ISP, Institute of Polar Science – National Research Council –via Torino, 155 - 30172 Venice-Mestre, Italy;
[4]Norwegian Polar Institute, Tromsø, Norway.
[5]University of Warsaw, Institute of Geophysics, Warsaw, Poland;
[6]Institute of Oceanology, Polish Academy of Sciences, Sopot, Poland;
[7]CNR-ISP, Institute of Polar Science – National Research Council – Via Gobetti 101, Bologna;
[8]Univ. Grenoble-Alpes, CNRS, IRD, Grenoble-INP, IGE, 38000 Grenoble, France

[#] Now at Laboratory of Atmospheric Chemistry, Paul Scherrer Institute, 5232 Villigen PSI, Switzerland

Abstract

Black Carbon (BC) is a major forcing agent in the Arctic but substantial uncertainty remains to quantify its climate effects due to the complexity of mechanisms involved. In this study, we provide unique information on processes driving the variability of BC mass concentration in surface snow in the Arctic. Two different snow-sampling strategies were adopted during spring 2014 and 2015, focusing on the *refractory* BC (rBC) mass Ny-Ålesund concentration daily/hourly variability on a seasonal/daily time scale (referred to as 80-days and 3-days experiments). Despite the low rBC mass concentrations (never exceeding 22 ng g^{-1}), a daily variability of up to 4.5 ng g^{-1} was observed. Atmospheric, meteorological and snow-related physico-chemical parameters were considered in multiple statistical models to understand the factors behind the observed variation of rBC mass concentrations. Results indicate that the main drivers of the variation of rBC are the precipitations events, snow metamorphism (melting-refreezing cycles, surface hoar formation and sublimation) and the activation of local sources (wind resuspension) during the snow melting periods. The rBC in the snow seems de-coupled with the atmospheric BC load. Our results highlighted a common association of snow rBC with coarse mode particles number concentration and with snow precipitation events.

https://doi.org/10.5194/acp-2020-574
Preprint. Discussion started: 8 July 2020

Atmospheric Chemistry and Physics Discussions

1. Introduction

In the last two decades, the Arctic regions have been exposed to dramatic changes in terms of atmospheric temperature rise, sea ice decreasing and increase of air mass transport from lower latitudes bringing warmer and humid air masses containing pollutants and anthropogenic derived compounds (Law and Stohl, 2007; Comiso et al., 2008; Screen and Simmonds, 2010; Eckhardt et al., 2013; Schmale et al., 2018; Maturilli et al., 2019). Despite a general decreasing trend observed in most parts of the globe, in the Arctic region the coefficients describing the aerosol optical properties, e.g. scattering and absorption, had generally shown a weakly increasing to a not-statistically significant trend (95% confidence), respectively (Collaud Coen et al., 2020). Long-range transport and local emissions of combustion generating aerosols as black carbon (BC) could influence the radiative budget of the Arctic atmosphere, especially after the impacts of atmospheric aging on the mixing state of BC particles (Eleftheriadis et al., 2009; Bond et al., 2013; Zanatta et al., 2018). When deposited over snow, many aerosol species directly absorb the solar radiation more efficiently than snow itself, thus favoring snow aging processes and the decrease of the snow albedo (Hansen and Nazarenko, 2004; Flanner et al., 2007; Hadley and Kirchstetter, 2012; Skiles et al., 2018; Skiles and Painter, 2019).

Among these light-absorbing aerosols, *black carbon* (BC) particles are the most effective in absorbing the visible and near infrared solar radiation. These primarily emitted, insoluble, refractory and carbonaceous particles originate from natural and anthropogenic sources such as open fires or diesel engine exhausts, respectively. Currently, the anthropogenic emissions are higher compared to the natural ones (Moosmüller et al., 2009; Bond et al., 2013). In 2000, approximately 59% of the total global BC emissions were generated from the energy production sector (including fossil fuels and solid residential fuels combustions) and the remaining from biomass burning (Bond et al., 2013). BC particles account for about 10% of the total aerosol mass in the European atmosphere and are characterized by a mass size distribution peaking around 100-250 nm (of mass equivalent diameter), e.g. at 240 nm in the Svalbard area in spring (Bond et al., 2013; Laborde et al., 2013; Zanatta et al., 2016; Motos et al., 2019). In a global perspective the BC radiative forcing (RF) is considered to be second only to that of CO_2, even though the value is characterized by a 90% uncertainty (Bond et al., 2013). The impact of BC particles absorbing the incoming solar radiation has certainly a non-negligible role in the Arctic region which is already threatened by a two-fold temperature increase compared to the mid-latitude regions, the so called "Arctic Amplification" (Bond et al., 2013; Cohen et al., 2014; Serreze and Barry, 2011). BC has an atmospheric lifetime of about seven days and has been directly targeted in important international mitigation agreements (Programme (AMAP), 2015). In this manuscript, the recommended nomenclature

https://doi.org/10.5194/acp-2020-574
Preprint. Discussion started: 8 July 2020


Atmospheric Chemistry and Physics Discussions

proposed in Petzold et al. (2013) is used to described the BC related quantities, depending on the deployed instrumental method.

Theoretical and experimental results showed that the cryosphere is affected both by the BC-induced warming of the atmosphere and by direct and indirect BC effects on the snow once deposited over it (Flanner, 2013), as for example the increase of absorbed incoming solar radiation by BC at snow surface. Consequently, snow is melting faster, decreasing the snow cover period, but snow is also aging more rapidly, which further decreases the snow albedo (Ramanathan and Carmichael, 2008; Brandt et al., 2011; Hadley and Kirchstetter, 2012).

Atmospheric BC measurements in the Arctic regions are still rare, despite an extraordinary effort done by the international scientific community in order to evaluate the sources, transport paths, concentration and climate impact (Eleftheriadis et al., 2009; Pedersen et al., 2015; Ferrero et al., 2016; Ruppel et al., 2017; Osmont et al., 2018; Zanatta et al., 2018; Laj et al., 2020). In order to understand the behavior of the BC particles in the snow mantle and to retrieve their radiative impact, several studies were performed in the last decades, measuring the amount of BC particles and their properties directly in the snow. A detailed list of previous measurements of BC in the Arctic snow pack (using different methodologies) is reported in Forsström et al. (2009) focused on snow surface in Svalbard and measured the *elemental carbon* (EC) content using filters and thermo/optical method. The results from 81 samples indicate a large variability in the EC mass concentration, ranges from 0 to about 80 ng g^{-1} (with a median mass concentration of about 4 ng g^{-1}). In Aamaas et al. (2011), the EC carbon mass concentration was measured in surface snow samples collected around the settlements of Longyearbyen and Svea in the Svalbard archipelago, that are affected by intense local sources (i.e. diesel, coal power plants and coal extraction). There, EC mass concentration in the snow samples was up to 1000 ng g^{-1}, rapidly decreasing with distance (50 ng g^{-1} at a distance of about 5 km). Oppositely, the snow collected near Ny-Ålesund was characterized by an average EC concentration of 6.6 ng g^{-1} with a standard deviation of 4.3 ng g^{-1}, defined as an Arctic background-like concentration. Moreover, Aamaas et al. (2011) observed that if the surface snow is influenced by melting episodes most of the BC-containing particles remain on the surface, therefore virtually increasing their mass concentration, especially during the spring season. Snow samples from Scandinavia and European Arctic were analyzed and discussed in Forsström et al. (2013) in terms of EC content: in the Scandinavian snow samples the EC concentrations were up to ~47 ng g^{-1}, due to local emissions, whereas in more remote regions as in Barrow (Northern Alaska) they were from 3 to 14 ng g^{-1}. The data discussed in Pedersen et al. (2015) from Arctic snow (Ny-Ålesund, Tromsø, Fram Strait and Barrow), also measured with the thermo-optical method were characterized by an EC concentration ranging from 5 to 137 ng g^{-1}. Specifically, the surface snow samples from Ny-Ålesund in

https://doi.org/10.5194/acp-2020-574
Preprint. Discussion started: 8 July 2020


Atmospheric Chemistry and Physics Discussions

2010 and 2011 had a median EC concentration from 18 to 21 ng g^{-1}. In Gogoi et al. (2016) snow samples were collected in the surrounding area of the atmospheric BC observatory at Gruvebadet (Ny-Ålesund, Svalbard) during April 2012. They used a filter based absorption method (Clarke and Noone, 1985), i.e. a dual wavelength optical transmissometer (Sootscan, Model OT-21, Magee Scientific, USA) at 880 and 370 nm. The *equivalent* BC (eqBC; derived from absorption measurements) mass concentrations in their samples ranged from 0.6 to 4.1 ng g^{-1}, and the fraction of BC from biomass burning was up to 25%. Khan et al. (2017) selected two sites, Woodfjorden and a coal dust contaminated site in southern Svalbard (Mine 7), to collect background-like and coal dust affected surface snow samples, respectively. Concentrations of EC varied from 5 to about 4000 ng g^{-1}. Also the refractory black carbon (rBC, i.e. measured with a Single Particle Soot Photometer – SP2, DMT) concentration values were reported ranging from 1 to 340 ng g^{-1}. The difference between the values obtained using the thermo-optical and the laser-induced incandesce (SP2) methods arises from the physical principles involved in the measurement, from the different size ranges and from differences in the aerosols physico-chemical characteristics. A review of the various methodologies to measure BC can be found in Bond et al. (2013), whereas a nomenclature definition in Petzold et al. (2013). Mori et al. (2019) analyzed the rBC mass concentration and size distribution for snow samples from several regions in the Arctic (Greenland, Finland, Alaska, Siberia, and Svalbard) showing a latitudinal variability, consistent with changes in anthropogenic BC emissions, atmospheric precipitable water content and topography changes.

A complex combination of processes are involved in the BC particles transfer from the atmosphere to the surface snow. The wet deposition is traditionally considered as the main scavenging process, particularly efficient for particles in the typical atmospheric BC size range. For bigger particles, instead, dry deposition is generally more efficient. Via a modelling approach, Liu et al. (2011) found that approximately 50% of the total burden of BC in the Arctic atmosphere is removed through wet deposition related processes. Yasunari et al. (2013) estimated the intensity of BC dry deposition on the Himalayan glaciers using several dry deposition methods (models and observations). Particularly, they found that the surface roughness and the surface wind speed are critical parameters in order to retrieve realistic results. Emerson et al. (2018) empirically evaluated the in situ rBC deposition velocities over a grassland (0.3 ± 0.2 mm s^{-1}), suggesting eddy covariance as the main deposition driver. In a recent study, Jacobi et al. (2019) confirmed the previous estimates of the importance of the wet deposition in removing BC particles in the atmosphere. Their results suggest that in spring and in the Svalbard Arctic area, approximately 60% of the BC particles are deposited on the surface snow via wet deposition. Moreover, they found out that the BC particles deposition is similar to those of nitrate and non-sea-salt (nss) sulfate, equally explained through wet and dry deposition (in contrast with the major sea salt components, mainly deposited via wet deposition).

https://doi.org/10.5194/acp-2020-574
Preprint. Discussion started: 8 July 2020


Atmospheric Chemistry and Physics Discussions

Complex air-snow BC transfer, post depositional processes and potentially high radiative impacts make the BC behavior in the Arctic snow pack an intriguing and complex research topic. BC content in the surface snow is still poorly characterized in the Arctic region, particularly for what concerns measurements performed with single-particle accurate instruments, i.e. the SP2. The absolute values of rBC mass concentration are important to evaluate the BC radiative impact via snow albedo reduction. In this work, the variability of the snow absolute rBC mass concentration was investigated for the first time following two different sampling frequencies, daily and hourly. To do this, two field campaigns were performed in the vicinity of the Gruvebadet Aerosol Laboratory, in Ny-Ålesund, during spring 2014 and 2015. The daily sampling lasted for approximately 80 days, allowing to evaluate the seasonal variability of BC. The daily sampling covered the transition from a cold period characterized by exceptionally frequent snow precipitation events to the melting period in late May, characterized by snow surface melting episodes and the presence of re-suspended surface material consequent to the collapse of the snow pack. In order to investigate the processes having a non-negligible role in regulating the surface snow rBC mass concentration, several parameters were deployed in a multilinear statistical model trying to explain the observed BC variability in the surface snow. Specifically, the statistical model took into account the atmospheric *equivalent* BC mass concentration, selected meteorological parameters, the snow coarse mode particles content and chemical parameters.

2. Experimental Methods

2.1 Study Area

Both experiments were conducted in the proximity of the Ny-Ålesund research station (78.5526 N, 11.5519 E, 25 m a.s.l.) located on the Spitzbergen island in the Svalbard Archipelago. Along the west coast, Svalbard is characterized by maritime climate with an annual average temperature of -3.9°C in Ny-Ålesund (between 1994 and 2017), and during that period, temperature increased by 1.6°C/decade (Maturilli et al., 2019). The measured mean annual temperatures for the years of the two campaigns described in this work were of -2.76°C (2014) and -2.16°C (2015). The average annual precipitation in Svalbard ranges from 190 to 525 mm (385 mm in Ny-Ålesund) with the highest precipitation rates occurring in August-October (mainly rain) and March, while May-June correspond to the lowest rates (Førland et al. 2011). During winter, snow covers most of the places and is the main interface influencing the ecosystem and climate system (Hansen et al. 2014). On average, the snow pack starts building up in September and melts away at the end of May (Førland et al. 2011). As reported in Maturilli et al. (2019), the year 2014 was characterized by the longest snow cover period, due to the exceptionally intense snow precipitation events.

https://doi.org/10.5194/acp-2020-574
Preprint. Discussion started: 8 July 2020


Atmospheric Chemistry and Physics Discussions

Snow samples were collected in the area close to the atmospheric research station of Gruvebadet (78.91734 N, 11.89535 E, 40 m a.s.l.), about 1 km South-West of Ny-Ålesund (Figure). Ny-Ålesund has become one of the reference locations for conducting Arctic climate studies focusing on atmospheric composition and physics, oceanography, biology, permafrost and snow-related activities as well as for evaluating the human impact in the higher Arctic. Long-term monitoring of atmospheric aerosols is performed at the Gruvebadet station (Feltracco et al., 2019; Moroni et al., 2018; Ferrero et al., 2016; Bazzano et al., 2015; Moroni et al., 2015; Zangrando et al., 2013; Scalabrin et al., 2012) as well as the Zeppelin observatory (475 m a.s.l.) (Eleftheriadis et al., 2009; Tunved et al., 2013; Lupi et al., 2016, and reference therein).

2.2 Snow Sampling

Snow samples were collected during two field campaigns: in spring 2014, from April 1 to June 24 (85 days in total, daily sampling, referred as "80-days") and in spring 2015 from April 28 to May 1 (three days, hourly sampling, referred as "3-days"). In the following, the two campaigns will be referred to as the 80-days and the 3-days experiment, respectively.

Two different sampling schemes were adopted regarding the thickness of the surface snow samples and the temporal sampling frequency. In the 80-days experiment, the first 10 cm of surface snow were collected on a daily basis (approximately at 11.00 am, GMT+2) in the same area, using a 5 cm diameter and 10 cm long Teflon tube. The snow samples were collected leaving a distance of approximately 15 cm between the previous sample location and following a straight line, in order to minimize the spatial variability influence. The collected snow was homogenized in a pre-cleaned plastic bag and then, without melting, a snow aliquot was transferred into a 50 mL vial (Falcon™ 50mL Conical Centrifuge Tubes) for BC, coarse mode particles number concentration and electrical conductivity analyses. On April 5, due to a snowstorm, the daily sample was not collected. During the 3-days experiment, the first 3 cm of surface snow were collected on an hourly basis in pre-cleaned vials in a delimited area of 2 m x 2 (Spolaor et al., 2019). To minimize the spatial variability, the samples have been collected following a straight line leaving about 5 cm between the sampling points. The samples for both experiments were kept frozen until the analyses period. The samples were collected using neck nylon gloves with particular attention to avoid any contamination from the not covered part and always downwind of the sampling area.

The temperature of the surface of the snow pack (at 7 cm for 80-days and at 3 cm for 3-days experiment) was always measured during the sampling with the same resolution. The daily/hourly snow accumulation was measured by using 4 poles placed around the sampling area as references. Temperature

https://doi.org/10.5194/acp-2020-574
Preprint. Discussion started: 8 July 2020


Atmospheric Chemistry and Physics Discussions

and accumulation measurements are ancillary data for evaluating snow deposition and ablation (precipitation/wind/melting).

2.3 Atmospheric Optical Measurements

2.3.1 Aethalometer (AE-31)

In this study, the equivalent BC (eBC) concentration in the lower atmosphere (around 3 m a.g.l) was measured by an AE-31 aethalometer (Gundel et al., 1983), during the 3-days campaign. The device is equipped with 7-wavelengths (370, 470, 520, 590, 660, 880, 950 nm) and determines the attenuation coefficient by using the ratio of light attenuated through a sensing spot (where aerosols are deposited) and a referenced clean spot, both on a quartz fiber filter substrate. The sampling and reference spots surface areas are 0.5 cm^2, while volumetric flow rate is 4 l min^{-1}. The flow rate was calibrated with a TetraCal (BGI Instruments) volumetric airflow before and after the field campaign. A 5 minutes temporal resolution was used for data acquisition. However, due to the low background concentration in the Arctic, the signal/noise ratio is high, so that data were average in an hour interval. Most of the filter-based techniques used to measure the aerosol absorption coefficient and eBC suffer from different systematic errors that must be corrected. In case of the aerosol absorption coefficient, the most important are the corrections for multiple scattering by the filter fibers and aerosol particles, and for filter loading effects. The data presented in this study were processed according to Segura et al. (2014) methodology. For this purpose the multiple scattering and filter loading effect (Weingartner et al., 2003) was corrected with new values of mass absorption cross section (MAC) and multiple scattering factor (C=3.1) reported by Zanatta et al. (2018). The MAC value was derived using observations and observationally constrained Mie calculations in spring at the Zeppelin Arctic station (Svalbard, 78°N). Zanatta et al. (2018) estimated the MAC at 550 nm (9.8 m2 g-1) and at 880 nm (6.95 m2 g-1), which we used to estimated MAC at 520 nm (10.2 m2 g-1).

2.3.2 Particle Soot Absorption Photometer (PSAP)

During the 80-days sampling period the aerosol absorption coefficient was also measured by means of a 3-wavelengths PSAP. It measures the variation of the transmission of light through a filter where particles are continuously deposited by a constant airflow. A second filter identical to the first one remains clean and is used as reference to take into account possible variations of the light source, i.e. a 3-color LED (blue, green and red with wavelength centered around 470, 530 and 670 nm, respectively). The correction developed by Bond et al. (1999) was applied to take into account the filter loading effect. The complete eBC mass concentration time series for the 80-days experiment was retrieved using the Aethalometer (first period) and the PSAP (second period), with an overlapping period with simultaneous

https://doi.org/10.5194/acp-2020-574
Preprint. Discussion started: 8 July 2020


Atmospheric Chemistry and Physics Discussions

measurements of 5 days. In order for the retrieved eBC mass concentration from the two instruments to be equal during the overlapping period, the PSAP eBC was calculated dividing the absorption measurements (at 530 nm) with a MAC equal to 7.25 m^2 g^{-1} (keeping the AE31 data as reference). From the 1-minute data, daily averages were calculated to compare with the rBC daily data obtained from the snow.

2.4 Surface Snow measurements

2.4.1 Coarse Mode Particles Number Concentration

The snow samples were melted at room temperature before the on-line coarse-mode particles and conductivity measurements (the water was pumped from the vials by a 12 channels peristaltic pump, ISMATECH, type ISM942). Specifically, the number concentration of coarse mode particles in the surface snow was measured with a Klotz Abakus laser sensor particles counter. This instrument optically counts the total number of particles and measures the size of each particles in a liquid constantly flowing through a laser beam cavity (LDS 23/23). The size range of this instrument is from 0.8 to about 80 µm with 32 dimensional bins (Table SI 1), not overlapping with that of the SP2. Only the 32nd bin has a dimensional range above 15.5 µm, i.e. of 80 µm. The data were recorded by a LabView® based software obtaining a sufficient number of data points in order to have a standard deviation of the mean smaller than 5%. The particles number concentration was calculated using the constant water flow value.

2.4.2 rBC Measurement – SP2

The rBC mass concentration and mass size distribution were measured following the methods described in Lim et al. (2014). Particularly, the snow samples were melted at room temperature prior to the analyses. The vials with the melted snow water were sonicated for ten minutes in water at room temperature. A glass nebulizer was used with filtered compressed air to nebulize the sample before the injection in the Apex-Q desolvation system (APEX-Q, Elemental Scientific Inc., Omaha, USA). The nebulization efficiency was evaluated daily by injecting Aquadag® solutions with different mass concentrations, ranging from 0.1 to 100 ng g^{-1}, obtaining an average value of 61%, that was used to correct all the BC mass concentrations reported in this manuscript. More details on the method can be found in Lim et al. (2014) and in Wendl et al. (2014).

A complete description of the theory of the SP2 functioning can be found in Stephens et al. (2003) and in Moteki and Kondo (2007) and Moteki and Kondo (2010). Briefly, the SP2 measurements are based on the laser-induced incandescence of the BC particles flowing through a high energy Nd-YaG laser with a wavelength of 1054 nm, at a single-particle level. The BC particles vaporize at about 4000 K emitting an incandescence signal proportional to their mass. The SP2 empirical calibration was performed using the standard reference fullerene soot (obtained from Alfa Aesar, stock #40971 and lot #FS12S011;

https://doi.org/10.5194/acp-2020-574
Preprint. Discussion started: 8 July 2020


Atmospheric Chemistry and Physics Discussions

the same used during the SP2 inter-comparison described in Laborde et al. (2012); Gysel et al. (2011)). During the calibration, the fullerene soot particles were size selected in terms of mobility diameter with a differential mobility analyzer (DMA), ranging from 80 to 500 nm. The calibration points were fitted using a linear fit. The mass equivalent diameter is calculated assuming the sphericity of the BC particles and an effective density of 1.8 g cm^{-3} (Moteki and Kondo, 2010).

The SP2 data were analyzed using the IGOR based toolkit from M. Gysel (Laboratory of Atmospheric Chemistry, Paul Scherrer Institute, Switzerland). The large amount of signals derived from every single particle are elaborated achieving rBC mass and number concentrations and size distributions. It's important to remark that the eBC and the rBC mass concentrations are not exactly the same physical quantities: the former is obtained from an absorption measurement assuming a constant MAC, whereas the second is obtained via a laser-induced-incandescence method with an SP2 empirically calibrated with a reference material (Petzold et al., 2013). Given the lack of a detailed mixing state characterization of the BC particles during the two experiments, it was not possible to predict or estimate the uncertainty introduced in the statistical analyses resulting from the two different measuring techniques. However, the statistical analyses are only related to the time variability of these two quantities and not to their absolute values.

2.4.3 Conductivity and sodium/manganese concentrations

The total conductivity of the melted snow was measured in parallel with a simple conductivity Micro-Cell. The water conductivity depends from the amount of soluble anions and cations in the snow, as for instance sea salt sodium. Concentrations of sodium (Na) and manganese (Mn) were also determined as tracer of sea spray emission and dust deposition by Inductively Coupled Plasma Sector Field Mass Spectrometry (ICP-SFMS; Element2, ThermoFischer, Bremen, Germany) equipped with a cyclonic Peltier-cooled spray chamber (ESI, Omaha, USA). The sample flow was maintained at 0.4 mL min^{-1}. Detection limits, calculated as three times the standard deviation of the blank, were 0.5 ng g^{-1} for ^{23}Na and 0.3 ng g^{-1} for Mn. The residual standard deviation (RSD) for Na and Mn ranged between 2–5%.

2.5 Meteorological Parameters

Several meteorological parameters have been used in the statistical exercise to relate the snow samples to the atmospheric conditions. Air temperature and relative humidity at 2 meter height have been retrieved from a meteorological station located about 800 meters north of the sampling site, using a ventilated PT-100 thermo-couple by Thies Clima and a HMT337 humicap sensor by Vaisala, respectively. Wind speed and direction at 10 meter height were obtained from a Combined Wind Sensor Classic by Thies Clima (see Maturilli et al., 2013). At about 50 m distance, the radiation measurements

https://doi.org/10.5194/acp-2020-574
Preprint. Discussion started: 8 July 2020


Atmospheric Chemistry and Physics Discussions

for the Baseline Surface Radiatio Network (BSRN) provide among others the downward solar radiation detected by a Kipp&Zonen CMP22 pyranometer (Maturilli et al., 2015). The meteorological and surface radiation measurements are available in a 1 minute time resolution via the PANGAEA data repository (Maturilli et al., 2020). The daily/hourly mean values of the meteorological parameters were used in the statistical analyses of the 80-days/3-days experiment and in Figure 2 and Figure 3 (the physico-chemical parameters from the snow samples are instead punctual value).

2.6 Statistical Analysis

Multiple linear regression was carried out to evaluate the associations between the observed surface snow rBC mass concentration and a set of predictors corresponding to the considered meteorological and snow physico-chemical parameters. The regression models describe variation in rBC concentrations as a function of atmospheric eBC concentration, surface snow coarse mode particles number concentration, snow internal temperature (7 cm depth for 80-days experiment and 2 cm depth for the 3-days experiment), snow precipitation, solar radiation and conductivity. The atmospheric concentration of eBC was included in the model as a potentially proxy to explain the rBC mass concentration in the surface snow. Other atmospheric parameters were initially considered, i.e. the wind speed and direction, and the atmospheric stability (expressed as vertical wind speed); however, they were removed because preliminary statistical analyses indicate that none of them is associated with the observed variations in snow rBC mass concentrations. The number concentration of coarse mode particles and the total electrical conductivity were included in the model in order to check common transport and deposition pathways and similarities/differences as a response to the snow melting. Snow temperature and the total incoming solar radiation were used to consider the thermodynamic processes occurring at the snow surface, as melting or condensation (surface hoar).

Since the predictors considered in the linear regression models for the two experiments are characterized by rather different measurement scales, results are reported in terms of standardized estimated coefficients obtained by fitting the regression model after standardizing the variables. The standardization simplifies the comparison among the different variables and between the two experiments, in this way facilitating the data interpretation and discussion.

Further details about the statistical analyses are given in the Supplementary material.

2.7 Back trajectories calculation and Potential Source Contribution Function analysis

Air mass back-trajectories (BT) were calculated using the NOAA ARL HYSPLIT 4 rev. 513 transport model (Stein et al., 2015). Global Data Assimilation System (GDAS) meteorological input fields with 0.5x0.5 degree resolution and a propagation time of 240 hours was employed. The trajectories

https://doi.org/10.5194/acp-2020-574
Preprint. Discussion started: 8 July 2020


Atmospheric Chemistry and Physics Discussions

were calculated every hour for an endpoint of 500 m above ground level in Ny-Ålesund. A potential source contribution function (PSCF) analysis has been applied to the BTs exploiting a specifically developed FORTRAN computer code (Petroselli et al., 2018). That analysis considered BC concentration measured in the air by both AE31 and PSAP. Briefly, the method calculates the probability of finding a source of a particular pollutant on a certain region by superimposing grid cells to it and estimating the fraction of the total time spent on each cell by trajectories associated with a high concentration measured at the receptor site. The 90th percentile was used to define the high concentration limit and cells of 3 x 3 degrees (lat-long) were exploited in the calculation of probabilities. Details of the PSCF methodology employed here are described in Petroselli et al., (2018). The data of the active fires, covering the last 12 days before the sampling day, are from the MODIS active fire products (https://firms.modaps.eosdis.nasa.gov/firemap/), offered by NASA LANCE.

3. Results and Discussions

3.1 Seasonal snow surface rBC variation

Seasonal rBC snow surface concentration changes were investigated for approximately 80 days. This experiment was performed in 2014 and covers approximately the entire spring periods until the snow pack melting. The results of the atmospheric measurements and from the analyses of the surface snow samples are reported in Figure2.

3.1.1 Atmospheric eBC concentrations

During the experiment period, the atmospheric eBC concentration show a remarkable variability ranging from 80 ng m^{-3} to < 5 ng m^{-3}. More in details, the highest concentrations were measured at the beginning of the campaign, especially from April 15 to 27, followed by a general decreasing trend characterized by the presence of several concentration peaks (on May 8, 17 and 24). Eurasian fires were suggested as the main source of biomass burning tracers during spring 2014 (Feltracco et al., 2020).

In order to evaluate the impact of the Eurasian fires on the measured atmospheric eBC concentrations, a thorough back-trajectories analysis was performed for both the snow-sampling periods. Results of PSCF analysis on eBC (Figures SI 1a, SI 1b and SI 1c; open-fire episodes are reported in red on the map) show a clear maximum of probability over the Central Siberia, which appears to be the major source area of eBC in this period over Ny-Ålesund. Some false positive source areas are located in Greenland, the Queen Elisabeth Islands region and the Arctic Ocean, even if associated to a lower probability. These artifacts are due to the persistent circulation of BTs in the Arctic vortex. An example of BTs generating the above salient features in the PSCF plot is reported in Figure SI 1b. Here BTs are shown to loop for few days around the Arctic at high altitudes and afterwards to descend at lower

https://doi.org/10.5194/acp-2020-574
Preprint. Discussion started: 8 July 2020


Atmospheric Chemistry and Physics Discussions

altitudes over Siberia, just four days before reaching Ny-Ålesund on April 22, when a clear maximum in the eBC trend has been recorded. Back trajectory analysis supports the idea that the peaks of eBC in the atmosphere in early spring are directly correlated with long-range transport from Eurasia, whereas the peaks in late May and June are much lower in intensity, seemed to be more related to a Western circulation pattern. The ammonia daily concentration time series (the only available biomass burning tracer for that period in the area) measured at the Zeppelin station is overlapped to the Gruvebadet atmospheric BC measurements in Figure SI 3. Biomass burning is known to be a significant source of atmospheric ammonia (Andreae and Merlet, 2001). As shown in Figure SI 3, the two time series have a similar behavior at the very beginning of the campaign, from April 3 to 8 and during the period between May 7 and 21.

3.1.2 Surface Snow/Atmospheric Aerosol Content and Atmospheric Conditions

During the 80-days sampling period, wind was characterized by the following median values (25th and 75th percentiles) of direction and speed: 205° (152°, 257°) and 2.7 (1.9, 3.7) m s^{-1}, respectively, therefore coming mostly from South-West (Figure). Daily air temperature increased during the campaign from -15°C to about +5°C (Figure 2), blue and red bars, represented as red bar in the legend), showing an average value and standard deviation of -3.5 ± 5.8 °C. The temperature increase followed the seasonal increase of the daily mean incoming solar radiation (Figure 2, orange line), increasing from approximately 100 to 300 W m^{-2}, with an average of 185 ± 75 W m^{-2}. The snow precipitation episodes are accounted for through the daily amount of deposited snow (Figure 2, blue bars), ranging from zero to 12 cm. The atmospheric eBC mass concentration, derived from the PSAP absorption coefficient, shows a decreasing trend during the campaign and a remarkable variability, ranging approximately from 2 to 80 ng m^{-3}, with an average of 34 ± 23 ng m^{-3}.

The snow rBC mass concentration shows a significant variability over the 80 days, ranging approximately from 0.2 to 6 ng g^{-1} (Figure 2), with an average of 1.4 ± 1.3 ng g^{-1}, and it is in agreement with results available in the literature (Mori et al., 2019; Jacobi et al., 2019; Aamaas et al., 2011). The spatial variability of BC was assumed to be comparable to the results described in Spolaor et al. (2019) for other particulate species in samples from the same field campaign. Nine samples were collected at the same time in the designed sampling area and the results show a spatial variability in the order of 5 to 15% (for sodium, mercury and iodine; Spolaor et al. (2019). An increasing trend can be observed for the rBC mass concentration in the surface snow during the sampling period. By comparing the observed values of this study with the results reported in Hadley and Kirchstetter (2012), we can estimate a very low snow albedo reduction due to the BC particles in our samples, always lower than approximately 0.01 (raw estimate). Given the low measured rBC mass concentrations, we decided not to calculate the BC radiative

https://doi.org/10.5194/acp-2020-574
Preprint. Discussion started: 8 July 2020


Atmospheric Chemistry and Physics Discussions

impact. Moreover, this study lacks any detailed description of the snow physical conditions, like the grain size, important for assessing realistic snow albedo reductions (Hadley and Kirchstetter, 2012; Skiles and Painter, 2019). The median of the rBC mass equivalent diameter in the snow is 313 ± 35 nm (Figure), similar to what obtained in other studies (e.g. Schwarz et al., 2013). The rBC mass equivalent diameter show high variability, ranging from 200 to 500 nm (however, since the rBC concentrations were low the evaluation of the particles geometric mean diameter for the biggest sizes, above 300/400 nm, has only to be considered as qualitative given the high noise in the size distributions).

The number concentration of coarse mode particles (Figure 2, blue line) shows a constant concentration in the first half of the campaign, until May 11, whereas increasing in the second half, especially after the 1st of June, in concomitance with the onset of the snow melting period; the average number concentration is 4914 ± 4109 # ml^{-1}. Also the conductivity (Figure 2, green line) shows an increasing trend at the end of the sampling campaign when snow is melting, with an overall average value of 30 ± 8 μS.

3.1.2 Variables explaining the snow rBC mass concentration variability

The fitted regression model for the 80-days experiment data explains 69% of the variance of snow rBC mass concentration (R2=0.69) and indicates a statistically significant association of the snow rBC mass concentration with the coarse-mode particles number concentration ($p < 0.001$), the amount of snow precipitations ($p < 0.05$) and the snow temperature ($p < 0.001$). The relations with the other predictors are non-significant (see Table 1, reporting the standardized estimated coefficients and the corresponding p-values). Figure 4 displays the 95% and 90% confidence intervals for the standardized estimated coefficients. Intervals that do not include the zero correspond to statistically significant predictors of the snow rBC mass concentration. If a confidence interval consists of positive values, then there is a significant positive association between the corresponding predictor and snow rBC mass concentration. Vice versa, if the confidence interval consists of negative values, then the association is negative. Figure 4 displays both the confidence intervals for the 80-days campaign and the 3-days experiment in a way to allow an immediate visual comparison of the estimated statistical associations between the snow rBC mass concentration and the considered predictors.

In order to interpret the statistical results, the description of the 80-days campaign is split into two periods depending on the temperature and the state of the snow. These periods identify the transition from the “cold” to the “melting” state. The first period occurred before the end of May: in this period the rBC mass concentration often increases in concomitance, or one day after, to most of the observed snowfall episodes (April 9/10/11 and 17; May 17, 22 and 27/28; June 1), with exceptions for April 24 and May 7. The sampling was performed in the late morning regardless the beginning/duration of the precipitation

https://doi.org/10.5194/acp-2020-574
Preprint. Discussion started: 8 July 2020


Atmospheric Chemistry and Physics Discussions

events. Over the sampling period, a weakly statistically significant ($p < 0.05$, Table 1) positive relation was found between snow rBC mass concentration in surface snow and the daily amount of snow precipitation. Given the complexity of the system, the short sampling period and daily frequency and the intrinsic internal variability, this positive association can only be tentatively linked to the BC wet deposition process, removing 50% - 60% of the total atmospheric BC burden in the Arctic (Liu et al., 2011; Jacobi et al., 2019). In our study, the impacts of the wet deposition could be partially masked due to the sampling frequency and timing. However, our observations show that, on a daily scale, the precipitation episodes are not clearly related to a decrease in the atmospheric eBC mass concentration (Figure 2). Nonetheless, a doubtful negative association was found in the fitted statistical model between the atmospheric eBC and snow rBC mass concentrations, with an associated p-value of 0.061.

In the second period, from the beginning of May on, the atmospheric temperature increases and the surface snow starts melting, inducing post-depositional effects on the snow impurities content. At the beginning of June, the snow rBC mass concentration increases up to approximately 5 ng g^{-1} and also the coarse mode particles number concentration increases remarkably (peaking between June 4 and 7). This positive relation is confirmed by the fitted regression model that indicates that the number of coarse mode particles is indeed the predictor with the highest significance level ($p < 0.001$, as reported in Table 1 and Figure 4). This positive relation can be explained by considering several processes affecting the BC and the coarse mode particles. Firstly, dry deposition is the main depositional process for the coarse mode particles, but recently it has been shown to be as well to provide a significant contribution in explaining the BC particles deposition (Liu et al., 2011; Jacobi et al., 2019). Secondly, it is possible that local sources become important contributors in the "melting" period due to the snow melting and the consequent exposure of soil and rocky areas in the surrounding of the sampling area. Ny-Ålesund was a mine town and the impact of local sources might have a non-negligible impact during the periods with little snow cover (autumns and late spring) and years with limited snow precipitations. Wind resuspension of BC (or other unknown refractory materials) and dust particles from uncovered areas eventually deposited on the remaining snow surfaces cause an acceleration of the melting and, as a consequence, a reduction of the snow season (positive feedback). The impacts of this positive feedback would be enhanced in a warmer climate where the activation of local sources would be longer in early winter and earlier in springtime.

Thirdly, we could explain the simultaneous increase of rBC mass and coarse mode particles number concentrations via post-depositional processes, as snow melting or sublimation, as visible between June 3 and 7-8. The episodes of snow surface melting can greatly affect the snow particulate content and we hypothesize that the hydrophobicity of pure BC particles, and of several species in the coarse mode particles, might affect its physical location in the snowpack during melting-refreezing

https://doi.org/10.5194/acp-2020-574
Preprint. Discussion started: 8 July 2020


Atmospheric Chemistry and Physics Discussions

episodes (in the literature the response of the BC particles is still debated): the hydrophobicity of the particles can cause the surface concentration to increase while losing water mass through percolation. Moreover, during the sublimation episodes, the losses of surface water mass lead to an increase of the particulate matter in the first layer of snow. The subsequent rBC mass and coarse mode particles number concentrations decrease can be speculatively explained with the complex behavior of the snow mantle during the strong melting and refreezing cycles and snow mantle collapsing. In conclusion, the processes causing the similar behavior observed in this study are complex to disentangle and full closure experiments are needed to tackle this subject, even though extremely complex and hardly manageable.

In this study, the estimated statistical association between snow rBC mass concentration and the daily snow temperature is negative and strongly significant ($p < 0.001$, Table 1 and Figure 4). During the 80 days experiment we can distinguish two events where the temperature appeared to play a role in the BC concentration, with an increase in rBC mass in the surface snow during the melting/refreezing episodes (in agreement with the results of Aamaas et al. (2011). The first event occurred between May 5 to 12 and the second after May 20, when the proper snow melting began (Figure 2). The first event was characterized by a rapid rise of daily air temperature (from -6°C to -1°C) in concomitance to a snow precipitation event, followed by a rapid temperature decrease to -6 °C. The surface snow (10 cm) mirrored this behavior first rising from -6 °C to 0°C and then cooling down to -6 °C. During this warm event, the upper snow strata underwent a melting with likely surface water percolation, making the surface BC concentration to increase. The second event started approximately on May 20 and lasted until the end of the experiment (Figure 2). During this period, the atmospheric temperature increased constantly, and the snow pack started to melt constantly. Moreover, surface BC concentration increased almost continuously from May 25 to its maximum observed in June 6. Afterwards, the upper snow rBC mass concentration tended to decrease following the rapid snow pack decline.

3.2 Diurnal variation of rBC in surface snow

3.2.1 Surface Snow/Atmospheric Aerosol Content and Atmospheric Conditions

The 3-days experiment was performed at the end of April 2015, during the Arctic spring. The samples were collected on an hourly basis over 3 days achieving a high-resolution sampling frequency. The wind direction and speed were quite constant (with median, 25th and 75th percentiles values of: 147°, 132°, 174° and 1.9, 1.4, 2.9 m s^{-1}, respectively) during the sampling period, blowing from South/Southeast or Southwest. The atmospheric and surface snow temperatures remained well below 0°C (Figure 3), with average values of -7.5 ± 1.2 °C and -8.3 ± 2.2 °C, respectively. The warmest air and snow temperature were approximately -5°C, therefore excluding surface snow melting to happen.

https://doi.org/10.5194/acp-2020-574
Preprint. Discussion started: 8 July 2020


Atmospheric Chemistry and Physics Discussions

504 The atmospheric concentration of eBC in ranged from 2 to 50 ng m^{-3}, decreasing during the
505 sampling period and not showing any particular diurnal pattern (Figure 3). The mean value of the
506 atmospheric eBC mass concentration is 34 ± 23 ng m^{-3}, similar to the average of the 80-days experiment.
507 The time series of the hourly eBC mass concentration is not showing any similar variability with snow
508 rBC time series, except for the common decreasing trend.
509 The surface snow rBC mass concentration exhibited hourly variability, showing up to 2-fold
510 hourly increases (especially during the first day), overlapped to a quasi-daily cycle (Figure 3, bottom
511 panel, smoothed dark blue line). rBC mass concentrations of approximately 15 ng g^{-1} were measured from
512 the beginning of the sampling to the end of the second day, and of about 5 ng g^{-1} from the beginning of
513 the third day till the end of experiment (Figure 3). The average value over the sampling period is 9.5 ± 5.2
514 ng g^{-1} (approximately 6 times higher than that during the 80-days experiment). This higher BC
515 concentrations are probably due to the limited number of snow episodes during this year, compared to the
516 year of the 80-days experiment, causing a higher impact of the dry BC deposition (before the snow
517 event). As reported for the 80-days experiment results, by considering the results from Hadley and
518 Kirchstetter (2012) it is possible to estimate a low snow albedo reduction of approximately 0.02-0.03
519 (difference between the albedo of pure snow and the albedo of snow with BC particles). Given the low
520 measured rBC mass concentrations, and the lack of detailed snow grain size measurements, we decided
521 not to calculate the BC radiative impact. Moreover, this study lacks any detailed description of the snow
522 physical conditions, as the grain size, important to assess realistic snow albedo reductions (Hadley and
523 Kirchstetter, 2012; Skiles and Painter, 2019). The rBC mass size distribution, instead, was characterized
524 by a median value of the geometric means of about 230 ± 32 nm, significantly lower than that which was
525 measured during the 80-days, and still in agreement with previous studies (Sinha et al., 2018; Bond et al.,
526 2013). The concentrations of EC and OC measured in parallel snow samples (not of the same volume) are
527 as well reported and described in Figure SI 4; the interpretation of the differences between the rBC and
528 the EC measurements in snow samples is beyond the objectives of this manuscript.
529 The number concentration of coarse mode particles remains virtually stable in the first half of the
530 campaign, until the end of April, and shows an average value over the whole three days of 26642 ± 9261
531 # ml^{-3} (approximately 5.5 times higher than during the 80-days experiment). The water conductivity
532 shows a similar behavior, and it is characterized by an average of 39 ± 9 µS (30% higher than during the
533 80-days experiment).
534 All the measured snow impurities time series show two common features: first, a decrease in
535 absolute values was detected between 4 and 8 a.m. of April 30, despite the absence of precipitations and
536 of any particular meteorological episode (Figure 3); second, the impact of the snow precipitation events
537 from approximately 4 p.m. to midnight of the April 30, where the concentrations of aerosols in the snow

https://doi.org/10.5194/acp-2020-574
Preprint. Discussion started: 8 July 2020


Atmospheric Chemistry and Physics Discussions

slightly increased at the very beginning whereas decreasing at the end of the event. Only the BC core diameter remained above the average when the other aerosol content decreased (up to approximately 400 nm of mass equivalent diameter), consequently going back to the average value. Also in this experiment, the spatial variability was estimated to account overall for the 5-15% to the total variability of the measured parameters (Spolaor et al., 2019).

The results of BT analysis for the 3-days experiment are reported in Figure SI 2, suggesting that the air masses were persistently circulating in the polar vortex and very similar within the three days in terms of BC atmospheric sources, physical properties and mixing state. The daily average concentration of ammonia, measured at the Zeppelin observatory, are similar to the lowest values measured during the 80-days experiment (approximately 0.5 μg L^{-1}), suggesting a background regime with a two-times increase during the last day (Figure SI 4). This result suggests what observed with the BT analyses: similar air masses during the sampling period with a low/negligible impact of the Northern Siberian fires (quite low in number during those days, Figure SI 2).

3.2.2 Variables explaining the snow rBC mass variability

The results obtained from the 3-days experiment have been evaluated using the same statistical approach considered to explain the rBC snow mass concentration variability in the 80-days experiment. The statistical model for the 3-days experiment explains 83% of the total snow rBC mass concentration variance, a percentage higher than the 80-days experiment, likely due to the more stable conditions. The fitted model indicates a statistically significant association between the rBC mass concentration in the snow and the conductivity ($p < 0.001$, Table 1), the number concentration of coarse-mode particles ($p < 0.01$, Table 1), the snow precipitation amount ($p < 0.001$, Table 1), the incoming solar radiation ($p < 0.01$, Table 1) and the snow temperature ($p < 0.05$, Table 1). The standardized estimated coefficients are reported in Table 1, displayed along with 90% and 95% confidence intervals in Figure 4.

The positive statistical association of total snow rBC mass concentration with the conductivity of the melted snow samples ($p < 0.001$, Table 1 and Figure 4) can be explained by a simultaneous deposition of different aerosol species (as sea salt with oceanic sources). For instance, air masses following pathways over the ocean after having entrained BC particles from biomass burning episodes will result in a positive correlation of snow BC and conductivity.

The association between the coarse-mode particles number concentration and the snow rBC mass concentration is positive and strongly significant ($p < 0.001$, Table 1 and Figure 4), similarly to what was observed for the 80-days experiment results.

A negative association is found between the rBC mass concentration in the snow and the incoming solar radiation ($p < 0.01$, Table 1 and Figure 4), and a weaker negative association with the

https://doi.org/10.5194/acp-2020-574
Preprint. Discussion started: 8 July 2020


Atmospheric Chemistry and Physics Discussions

snow temperature ($p < 0.05$, Table 1 and Figure 4), with the latter being strongly dependent on the solar radiation. This relation confirms what observed in Figure 3: the rBC mass concentration in surface snow follows a diurnal cycle, lower when the solar radiation is higher and vice versa. The quasi-daily cycle of rBC mass concentration in the surface snow layer has never been studied and reported in the literature. The BC particles are known to be non-volatile and non-photochemical active, therefore the decrease in its concentration observed when the solar radiation is higher could not be explained as a re-emission process from the snow back into the atmosphere as observed for other aerosol species (Spolaor et al., 2018; Spolaor et al., 2019). The results show that the highest rBC mass concentration levels are detected in samples collected in the late afternoon. The late night/early morning concentration decrease is connected with surface hoar formation able to dilute the surface snow BC concentration. Specifically, the lowest rBC mass concentration values is found between 5 and 12 am and in the same time interval the solar radiation increases from 100 to 400 W m^{-2}, followed with a delay by air and snow temperatures increase. In these periods, the temperature offset between the air and the surface snow is the highest, up to 4°C, with the surface snow being the coldest between the two. Condensation of water vapor on the top of the snow crystals is possible, adding snow mass without BC in the collected samples and diluting the original rBC mass concentration. This process may lead to an overall negative feedback on the BC radiative impact, making its concentration to decrease during the daily maximum of solar radiation.

The snow precipitation amount is negatively associated with the rBC mass concentration in the snow ($p < 0.001$, Table 1 and Figure 4). As previously remarked, the aerosol scavenging intensity is not measurable with snow sampling strategies based on the sampling of a constant snow thickness from the surface (3 cm in this case). The negative relation observed in this study is due to the high frequency sampling, being able to follow the evolution of the BC particles scavenged during a snow episode (from 3 to 12 p.m. of the 30th April 2015). The beginning of the precipitation episodes appeared to remove the highest amount of BC particles, leaving the atmosphere cleaner as reflected by the lower BC mass concentration revealed in subsequent samples. The snow collected at 18:00 of April 30 showed a higher amount of rBC as well as the highest coarse mode particles number concentration and conductivity. In the next few hours, from 9 to 12 p.m., the snow precipitations were very "clean" in terms of aerosol content and rBC mass concentration.

From the 3-days experiment, it appeared that the snow surface physical processes like surface hoar formation and sublimation play an important role, and that the physical characteristics of the snow layers in which BC is embedded should be more studied in order to better characterize the daily variations of BC and its impact on the albedo. The 3 days experiment took place under clear sky conditions (most of the time) and this is of high importance for the variations observed. Indeed, surface hoar can only form under clear sky when the snow surface is cooler than the air due to longwave radiation emitted and lost,

https://doi.org/10.5194/acp-2020-574
Preprint. Discussion started: 8 July 2020


Atmospheric Chemistry and Physics Discussions

and under calm weather with low wind. Under other conditions, cloudy weather for example, the BC diurnal variation may show a completely different pattern, as snow will likely be affected by longwave radiation backscattered by clouds toward the snow surface, and melting and/or sublimation at the snow surface will only be observed, but likely no condensation of atmospheric water vapor. Furthermore, these daily variations showed that the highest concentration of rBC is measured during mid-day/afternoon, when the incoming radiation amount is still high, and that may significantly affect the amount of extra energy absorbed by the surface snow, further enhancing metamorphism and feedback processes. More detailed studies including snow density and optical snow grain radius measurements should be pursued and at a cm vertical resolution in order to correctly estimate the radiative impact of the daily rBC variations.

4. Conclusions and Future Perspectives

The two experiments suggested that the main drivers of the rBC mass concentration variation in the Svalbard surface snow are mainly precipitations events, snow metamorphism (melting and surface hoar formation and sublimation), and potentially the activation of local sources during the melting periods triggering a positive-feedback based on the snow albedo reduction. On a daily frequency (80-days experiment) coarse-mode particles are associated to the snow rBC mass concentration, even in periods characterized by the influence of biomass burning emissions. On an hourly frequency (3-days experiment) the snow deposition and the daily solar radiation cycle appeared to be mostly controlling the surface snow rBC content under clear sky, via hoar formation/condensation processes, with the coarse mode particles number concentration positively associated with it. The absolute rBC mass concentration resulting in a minor or negligible snow albedo reduction of approximately the 3% at maximum (see Hadley and Kirchstetter, 2012).

During the seasonal time scale (daily sampling strategy), the multilinear statistical model was able to explain 69% of the surface snow rBC mass concentration variance. Our results indicate a positive association between the snow rBC mass concentration and the coarse-mode particles number concentration, due to similar responses to dry and wet deposition processes and comparable behaviors in the presence of post-depositional processes. The amount of rBC in the surface snow appeared to be statistically de-coupled from the eBC atmospheric load. The importance of the wet-deposition process was statistically highlighted in both experiments.

Long-range transport and melting-induced activation of local sources are key parameters in describing the BC origin in the atmosphere and in the surface snow in the Ny-Ålesund area (and might in a large portion of the Svalbard archipelago), acting with different intensities during the year. However, our results suggest that despite possible high atmospheric BC concentrations as in the case of long-range

https://doi.org/10.5194/acp-2020-574
Preprint. Discussion started: 8 July 2020


Atmospheric Chemistry and Physics Discussions

transport of biomass burning plumes, the surface snow rBC mass concentration can be almost completely unaffected in the absence of snow precipitation events. During the surface snow melting period (with atmospheric temperatures above 0°C) we revealed an increase of snow rBC mass and coarse-mode particles number concentrations, suggesting an increase of the impact of the local sources, activated by the snow melting leaving the surface exposed to winds. Moreover, this measured increase in the snow aerosol load is influenced by the response to melting-refreezing cycles and water mass loss. Both these mechanisms cause an increase in the snow surface insoluble particles concentration, causing a positive-feedback mechanism enhancing their radiative impacts and fastening the snow melting.

83% of the hourly/daily variance was explained by the statistical model, again resulting in a positive association with the coarse-mode particles number concentration, suggesting similar responses to the depositional patterns and responses to post depositional processes (condensation of water vapor on the top of the snow crystals). The negative association with the solar radiation and the temperature of the snow suggest that part of the rBC mass variability in the snow undergoes to a daily cycle linked to snow metamorphism processes, as sublimation and condensation of atmospheric water vapor. The condensation of water vapor on the upper layer of the snow makes the rBC mass concentration decrease by dilution (when keeping a constant sampling thickness), especially during the hours of the day when the solar radiation is at its maximum: however, the complex snow crystals-radiation interaction makes it difficult to evaluate the radiative impact of this process.

Acknowledgements

This work was part of the PhD (in “Science and Management of Climate Change”) of Michele Bertò at the Ca’ Foscari University of Venice that was partly funded with the Early Human Impact ERC project. Thanks to Giuseppe Pellegrino for helping collecting the samples. Thanks to Jacopo Gabrieli and the technicians of the Ca’Foscari University of Venice for the precious help in building up the coarse mode particles and conductivity measurement apparatus. We acknowledge the use of data and imagery from LANCE FIRMS operated by the NASA/GSFC/Earth Science Data and Information System (ESDIS) with funding provided by NASA/HQ. We want to thank Paolo Laj and the LGGE (Grenoble, France) for lending us the SP2 and Marco Zanatta for transferring the SP2 know-how on instrumental functioning and data analyses. Thanks to Martin Gysel-Beer, PSI, for the IGOR based SP2 Toolkit for SP2 data analyses. We thank Marion Maturilli and AWI for providing us with the meteorological data. Thanks to Giorgio Bertò for checking and correcting the language of this manuscript. This paper is an output of the AMIS project in the framework of “Project MIUR – Dipartimenti di Eccellenza 2018-2022”. This project has received funding from the European Union's Horizon 2020 research and innovation programme under

https://doi.org/10.5194/acp-2020-574
Preprint. Discussion started: 8 July 2020

grant agreement No 689443 via project iCUPE (Integrative and Comprehensive Understanding on Polar Environments).

Data Availability

Meterological and surface radiation data are available at the PANGAEA database (Maturilli, 2015a; 2015b; 2015c; 2016a; 2016b; 2018a; 2018b; 2018c; 2018d; 2018e). The data for precipitation amount at Ny-Ålesund can be accessed via the eKlima database of MET Norway. The BC data are available upon request.

Author Contributions

Author contributions. AS, EB, DC and MB conceived the experiments; AS, EB, DC, and LP collected the samples; MB measured the samples; KM and MMaz provided the atmospheric eBC concentrations; SC and DC provided the back-trajectories analyses; CV performed the statistical analyses with inputs from MB and AS. MB prepared the manuscript mainly with inputs from AS, J-C. G and DC (in the methods section from AS, KM, MMaz) and all co-authors contributed to the interpretation of the results as well as manuscript review and editing.

Data repository

Maturilli, Marion (2020): Basic and other measurements of radiation and continuous meteorological observations at station Ny-Ålesund (April, May 2014 and April, May, June 2015), reference list of 10 datasets. Alfred Wegener Institute - Research Unit Potsdam, PANGAEA, https://doi.pangaea.de/10.1594/PANGAEA.913988 (DOI registration in progress)

https://doi.org/10.5194/acp-2020-574
Preprint. Discussion started: 8 July 2020

Atmospheric Chemistry and Physics Discussions

703 **FIGURES**

704 **Figure 1.** a) Experimental sampling site location (dark grey rectangle), in proximity of the Gruvebadet
705 Aerosol Laboratory. b) Gruvebadet area (black square), close to the Ny-Ålesund research village. From:
706 Spolaor et al., 2019 (maps from https://toposvalbard.npolar.no/)

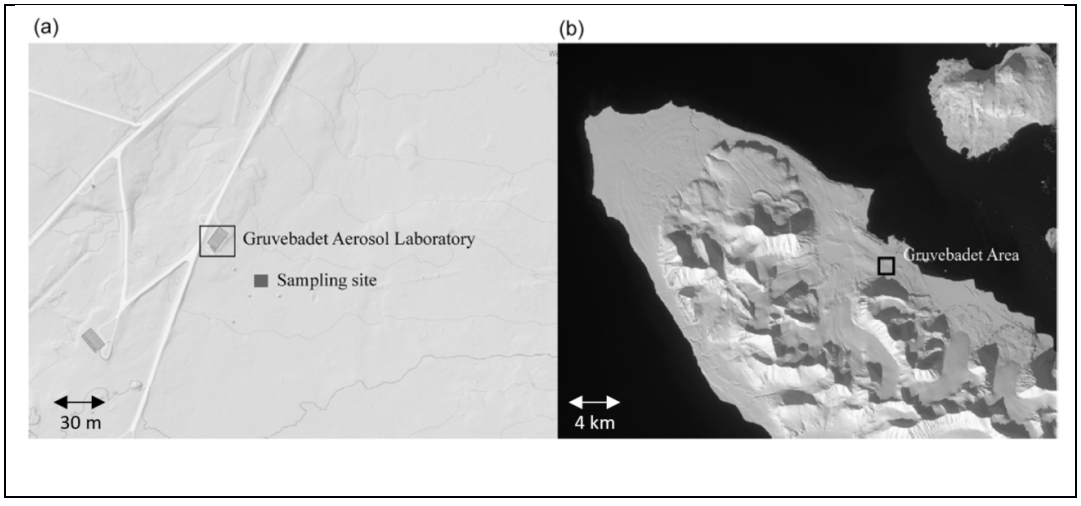

707

708

709

710

711

712

713

714

715

716

717

718

https://doi.org/10.5194/acp-2020-574
Preprint. Discussion started: 8 July 2020

Atmospheric Chemistry and Physics Discussions

719 **Figure 2.** The 80-days experiments daily snow samples rBC mass concentration (light blue), eBC mass
720 concentration in the atmosphere (black), geometric mean mass equivalent diameter (purple), number of
721 coarse mode particles (blue), total conductivity (green), meteo/snow parameters used in the statistical
722 exercise: wind speed color coded for wind direction, solar radiation (orange line), air and surface snow
723 temperatures (blue bars and green line respectively), amount of fresh snow ("snow precipitations", light
724 blue bars) and the snow accumulation ("Neg. accumulation"; the values where multiplied by -1 in order to
725 show the similar trend of the snow lost and of the air/snow temperature during the melting period at the
726 end of the campaign).

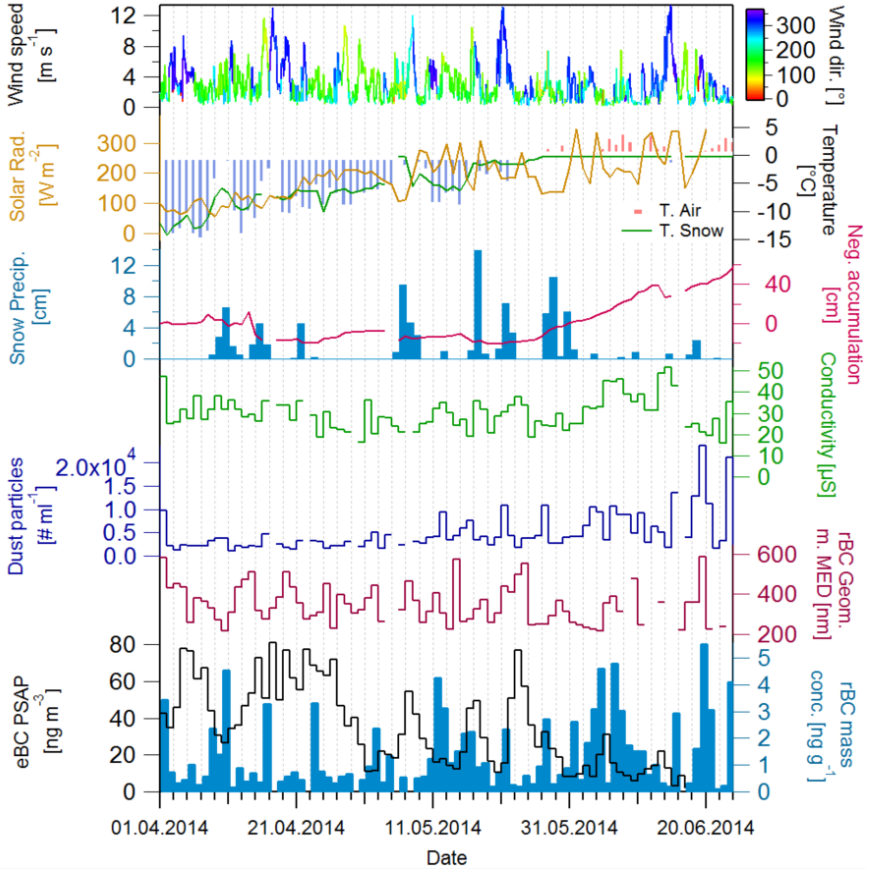

727

728

729

https://doi.org/10.5194/acp-2020-574
Preprint. Discussion started: 8 July 2020

Atmospheric Chemistry and Physics Discussions

730 **Figure 3.** The 3-days experiments snow samples hourly rBC mass concentration and smoothed line (light
731 blue bars), atmospheric eBC mass concentration in the atmosphere (black), geometric mean mass
732 equivalent diameter (purple), the number concentration of coarse mode particles (blue) and the total
733 conductivity (green), meteo/snow parameters used in the statistical exercise: wind speed color coded for
734 wind direction, solar radiation (Orange line), Air and surface snow temperature (blue bars and green line
735 respectively), amount of fresh snow ("snow precipitations", light blue bars). The yellow bars are centered
736 on the midnight hours for the three sampling days.

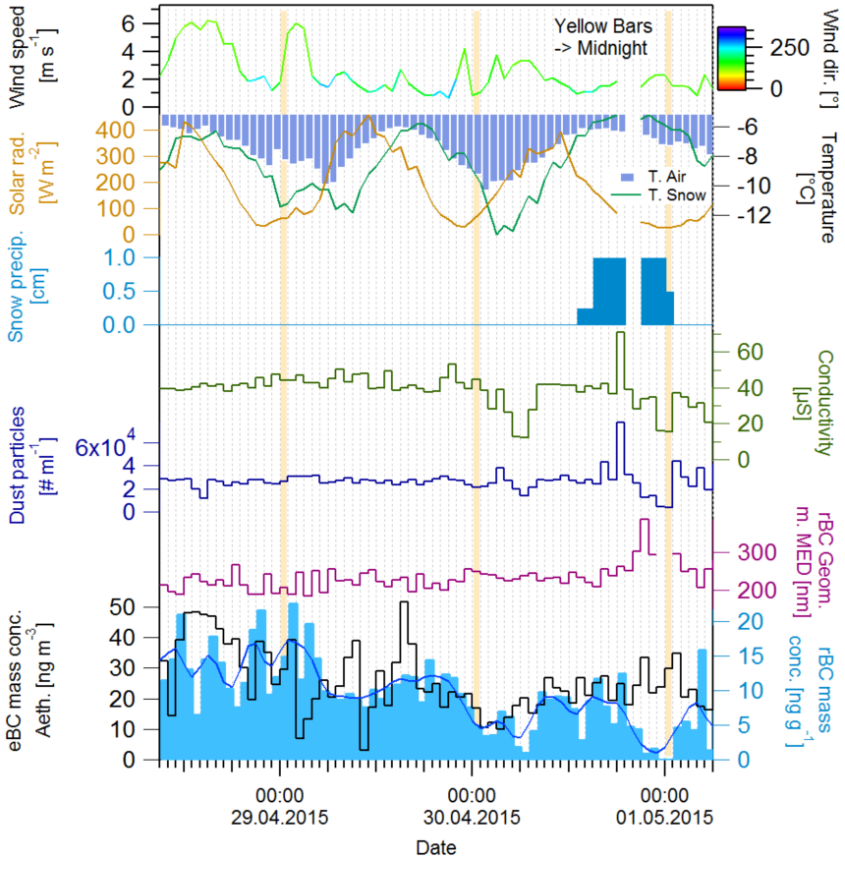

737

738

739

740

https://doi.org/10.5194/acp-2020-574
Preprint. Discussion started: 8 July 2020

Atmospheric Chemistry and Physics Discussions

741 **Figure 4.** Standardized estimated coefficients of the multiple regression models fitted to the 3 days and
742 80 days experiments. The segments correspond to 95% confidence intervals about the corresponding
743 estimates. The internal thicker segments correspond to 90% confidence intervals. The abbreviations used
744 in the plot are: "log(cond)" – logarithm of the water conductivity time series, "log(dust)" – logarithm of
745 the coarse mode particles number concentration time series, "eBC" – equivalent black carbon atmospheric
746 concentration, "snow" – amount of fresh snow from the precipitation episodes, "SWR" – solar radiation,
747 "temp" – the snow temperature.

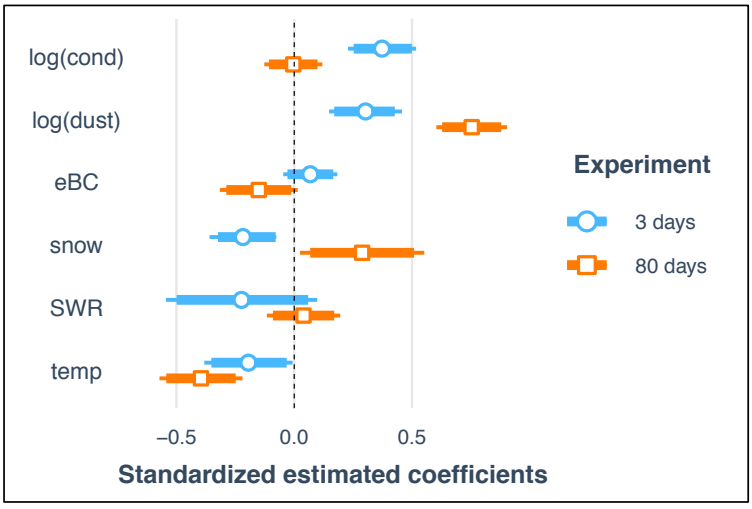

748
749
750
751
752
753
754
755
756

https://doi.org/10.5194/acp-2020-574
Preprint. Discussion started: 8 July 2020

Atmospheric Chemistry and Physics Discussions

TABLES

Table 1. Standardized estimated coefficients of the regression models for the 3 days and 80 days experiments. Standard errors are reported within parentheses below the corresponding estimate. The intercept and the trigonometric terms are not displayed.

Predictor	3 days	80 days
log(cond)	0.38 ***	-0.00
	(0.07)	(0.06)
log(dust)	0.23 **	0.75 ***
	(0.07)	(0.08)
eBC	0.06	-0.15
	(0.05)	(0.08)
snow	-1.02 ***	0.29 *
	(0.19)	(0.13)
SWR	-0.43 **	0.04
	(0.16)	(0.08)
temp	-0.23 *	-0.40 ***
	(0.09)	(0.09)
R^2	0.83	0.69

*** **p** < 0.001; ** **p** < 0.01; * **p** < 0.05

https://doi.org/10.5194/acp-2020-574
Preprint. Discussion started: 8 July 2020

Atmospheric Chemistry and Physics Discussions

References

Aamaas, B., Bøggild, C. E., Stordal, F., Berntsen, T., Holmèn, K. and Strùm, J.: Elemental carbon deposition to Svalbard snow from Norwegian settlements and long-range transport, Tellus B Chem. Phys. Meteorol., 63(3), 340–351, doi:10.1111/j.1600-0889.2011.00531.x, 2011.

Andreae, M. O. and Merlet, P.: Emission of trace gases and aerosols from biomass burning, Glob. Biogeochem. Cycles, 15(4), 955–966, doi:10.1029/2000GB001382, 2001.

Bazzano, A., Ardini, F., Becagli, S., Traversi, R., Udisti, R., Cappelletti, D. and Grotti, M.: Source assessment of atmospheric lead measured at Ny-Ålesund, Svalbard, Atmos. Environ., 113, 20–26, doi:10.1016/j.atmosenv.2015.04.053, 2015.

Bond, T. C., Anderson, T. L. and Campbell, D.: Calibration and Intercomparison of Filter-Based Measurements of Visible Light Absorption by Aerosols, Aerosol Sci. Technol., 30(6), 582–600, doi:10.1080/027868299304435, 1999.

Bond, T. C., Doherty, S. J., Fahey, D. W., Forster, P. M., Berntsen, T., DeAngelo, B. J., Flanner, M. G., Ghan, S., Kärcher, B., Koch, D., Kinne, S., Kondo, Y., Quinn, P. K., Sarofim, M. C., Schultz, M. G., Schulz, M., Venkataraman, C., Zhang, H., Zhang, S., Bellouin, N., Guttikunda, S. K., Hopke, P. K., Jacobson, M. Z., Kaiser, J. W., Klimont, Z., Lohmann, U., Schwarz, J. P., Shindell, D., Storelvmo, T., Warren, S. G. and Zender, C. S.: Bounding the role of black carbon in the climate system: A scientific assessment: BLACK CARBON IN THE CLIMATE SYSTEM, J. Geophys. Res. Atmospheres, 118(11), 5380–5552, doi:10.1002/jgrd.50171, 2013.

Brandt, R. E., Warren, S. G. and Clarke, A. D.: A controlled snowmaking experiment testing the relation between black carbon content and reduction of snow albedo, J. Geophys. Res. Atmospheres, 116(D8), doi:10.1029/2010JD015330, 2011.

Clarke, A. D. and Noone, K. J.: Soot in the Arctic snowpack: a cause for perturbations in radiative transfer, Atmospheric Environ. 1967, 19(12), 2045–2053, doi:10.1016/0004-6981(85)90113-1, 1985.

Cohen, J., Screen, J. A., Furtado, J. C., Barlow, M., Whittleston, D., Coumou, D., Francis, J., Dethloff, K., Entekhabi, D., Overland, J. and Jones, J.: Recent Arctic amplification and extreme mid-latitude weather, Nat. Geosci., 7(9), 627–637, doi:10.1038/ngeo2234, 2014.

Collaud Coen, M., Andrews, E., Alastuey, A., Arsov, T. P., Backman, J., Brem, B. T., Bukowiecki, N., Couret, C., Eleftheriadis, K., Flentje, H., Fiebig, M., Gysel-Beer, M., Hand, J. L., Hoffer, A., Hooda, R., Hueglin, C., Joubert, W., Keywood, M., Kim, J. E., Kim, S.-W., Labuschagne, C., Lin, N.-H., Lin, Y., Lund Myhre, C., Luoma, K., Lyamani, H., Marinoni, A., Mayol-Bracero, O. L., Mihalopoulos, N., Pandolfi, M., Prats, N., Prenni, A. J., Putaud, J.-P., Ries, L., Reisen, F., Sellegri, K., Sharma, S., Sheridan, P., Sherman, J. P., Sun, J., Titos, G., Torres, E., Tuch, T., Weller, R., Wiedensohler, A., Zieger, P. and Laj, P.: Multidecadal trend analysis of aerosol radiative properties at a global scale, Atmospheric Chem. Phys. Discuss., 1–54, doi:https://doi.org/10.5194/acp-2019-1174, 2020.

Comiso, J. C., Parkinson, C. L., Gersten, R. and Stock, L.: Accelerated decline in the Arctic sea ice cover, Geophys. Res. Lett., 35(1), doi:10.1029/2007GL031972, 2008.

Eckhardt, S., Hermansen, O., Grythe, H., Fiebig, M., Stebel, K., Cassiani, M., Baecklund, A. and Stohl, A.: The influence of cruise ship emissions on air pollution in Svalbard - a harbinger of a more polluted

https://doi.org/10.5194/acp-2020-574
Preprint. Discussion started: 8 July 2020

Atmospheric Chemistry and Physics Discussions

808 Arctic?, Atmospheric Chem. Phys., 13(16), 8401–8409, doi:https://doi.org/10.5194/acp-13-8401-2013,
809 2013.

810 Eleftheriadis, K., Vratolis, S. and Nyeki, S.: Aerosol black carbon in the European Arctic: Measurements
811 at Zeppelin station, Ny-Ålesund, Svalbard from 1998–2007, Geophys. Res. Lett., 36(2),
812 doi:10.1029/2008GL035741, 2009.

813 Emerson, E. W., Katich, J. M., Schwarz, J. P., McMeeking, G. R. and Farmer, D. K.: Direct
814 Measurements of Dry and Wet Deposition of Black Carbon Over a Grassland, J. Geophys. Res.
815 Atmospheres, 123(21), 12,277-12,290, doi:10.1029/2018JD028954, 2018.

816 Feltracco, M., Barbaro, E., Kirchgeorg, T., Spolaor, A., Turetta, C., Zangrando, R., Barbante, C. and
817 Gambaro, A.: Free and combined L- and D-amino acids in Arctic aerosol, Chemosphere, 220, 412–421,
818 doi:10.1016/j.chemosphere.2018.12.147, 2019.

819 Feltracco, M., Barbaro, E., Tedeschi, S., Spolaor, A., Turetta, C., Vecchiato, M., Morabito, E.,
820 Zangrando, R., Barbante, C. and Gambaro, A.: Interannual variability of sugars in Arctic aerosol:
821 Biomass burning and biogenic inputs, Sci. Total Environ., 706, 136089,
822 doi:10.1016/j.scitotenv.2019.136089, 2020.

823 Ferrero, L., Cappelletti, D., Busetto, M., Mazzola, M., Lupi, A., Lanconelli, C., Becagli, S., Traversi, R.,
824 Caiazzo, L., Giardi, F., Moroni, B., Crocchianti, S., Fierz, M., Mocnik, G., Sangiorgi, G., Perrone, M.
825 G., Maturilli, M., Vitale, V., Udisti, R. and Bolzacchini, E.: Vertical profiles of aerosol and black carbon
826 in the Arctic: a seasonal phenomenology along two years (2011-2012) of field campaign, Atmospheric
827 Chem. Phys., 16, 12601–12629, doi: https://doi.org/10.5194/acp-16-12601-2016
828 <https://doi.org/10.5194/acp-16-12601-2016> , hdl:10013/epic.48736, 2016.

829 Flanner, M. G.: Arctic climate sensitivity to local black carbon, J. Geophys. Res. Atmospheres, 118(4),
830 1840–1851, doi:10.1002/jgrd.50176, 2013.

831 Flanner, M. G., Zender, C. S., Randerson, J. T. and Rasch, P. J.: Present-day climate forcing and response
832 from black carbon in snow, J. Geophys. Res. Atmospheres, 112(D11), doi:10.1029/2006JD008003,
833 2007.

834 Forsström, S., Ström, J., Pedersen, C. A., Isaksson, E. and Gerland, S.: Elemental carbon distribution in
835 Svalbard snow, J. Geophys. Res. Atmospheres, 114(D19), doi:10.1029/2008JD011480, 2009.

836 Forsström, S., Isaksson, E., Skeie, R. B., Ström, J., Pedersen, C. A., Hudson, S. R., Berntsen, T. K.,
837 Lihavainen, H., Godtliebsen, F. and Gerland, S.: Elemental carbon measurements in European Arctic
838 snow packs, J. Geophys. Res. Atmospheres, 118(24), 13,614-13,627, doi:10.1002/2013JD019886, 2013.

839 Gogoi, M. M., Babu, S. S., Moorthy, K. K., Thakur, R. C., Chaubey, J. P. and Nair, V. S.: Aerosol black
840 carbon over Svalbard regions of Arctic, Polar Sci., 10(1), 60–70, doi:10.1016/j.polar.2015.11.001, 2016.

841 Gundel, L. A., Dod, R. L., Rosen, H. and Novakov, T.: Relationship between optical attenuation and
842 black carbon concentration for ambient and source particles, Lawrence Berkeley Lab., CA (USA).
843 [online] Available from: https://www.osti.gov/biblio/5653266 (Accessed 7 May 2020), 1983.

844 Gysel, M., Laborde, M., Olfert, J. S., Subramanian, R. and Gröhn, A. J.: Effective density of Aquadag
845 and fullerene soot black carbon reference materials used for SP2 calibration, Atmospheric Meas. Tech.,
846 4(12), 2851–2858, doi:https://doi.org/10.5194/amt-4-2851-2011, 2011.

https://doi.org/10.5194/acp-2020-574
Preprint. Discussion started: 8 July 2020

Atmospheric Chemistry and Physics Discussions

847 Hadley, O. L. and Kirchstetter, T. W.: Black-carbon reduction of snow albedo, Nat. Clim. Change, 2(6),
848 437–440, doi:10.1038/nclimate1433, 2012.

849 Hansen, J. and Nazarenko, L.: Soot climate forcing via snow and ice albedos, Proc. Natl. Acad. Sci.,
850 101(2), 423–428, doi:10.1073/pnas.2237157100, 2004.

851 Jacobi, H.-W., Obleitner, F., Da Costa, S., Ginot, P., Eleftheriadis, K., Aas, W. and Zanatta, M.:
852 Deposition of ionic species and black carbon to the Arctic snowpack: combining snow pit observations
853 with modeling, 10361-10377, doi:10.5194/acp-19-10361-2019, 2019.

854 Khan, A. L., Dierssen, H., Schwarz, J. P., Schmitt, C., Chlus, A., Hermanson, M., Painter, T. H. and
855 McKnight, D. M.: Impacts of coal dust from an active mine on the spectral reflectance of Arctic surface
856 snow in Svalbard, Norway, J. Geophys. Res. Atmospheres, 122(3), 1767–1778,
857 doi:10.1002/2016JD025757, 2017.

858 Laborde, M., Schnaiter, M., Linke, C., Saathoff, H., Naumann, K. H., Möhler, O., Berlenz, S., Wagner,
859 U., Taylor, J. W., Liu, D., Flynn, M., Allan, J. D., Coe, H., Heimerl, K., Dahlkötter, F., Weinzierl, B.,
860 Wollny, A. G., Zanatta, M., Cozic, J., Laj, P., Hitzenberger, R., Schwarz, J. P. and Gysel, M.: Single
861 Particle Soot Photometer intercomparison at the AIDA chamber, Atmos Meas Tech, 22, 2012.

862 Laborde, M., Crippa, M., Tritscher, T., Jurányi, Z., Decarlo, P. F., Temime-Roussel, B., Marchand, N.,
863 Eckhardt, S., Stohl, A., Baltensperger, U., Prévôt, A. S. H., Weingartner, E. and Gysel, M.: Black
864 carbon physical properties and mixing state in the European megacity Paris, Atmospheric Chem. Phys.,
865 13(11), 5831–5856, doi:10.5194/acp-13-5831-2013, 2013.

866 Laj, P., Bigi, A., Rose, C., Andrews, E., Lund Myhre, C., Collaud Coen, M., Wiedensohler, A., Schultz,
867 M., Ogren, J. A., Fiebig, M., Gliß, J., Mortier, A., Pandolfi, M., Petäjä, T., Kim, S.-W., Aas, W., Putaud,
868 J.-P., Mayol-Bracero, O., Keywood, M., Labrador, L., Aalto, P., Ahlberg, E., Alados Arboledas, L.,
869 Alastuey, A., Andrade, M., Artíñano, B., Ausmeel, S., Arsov, T., Asmi, E., Backman, J., Baltensperger,
870 U., Bastian, S., Bath, O., Beukes, J. P., Brem, B. T., Bukowiecki, N., Conil, S., Couret, C., Day, D.,
871 Dayantolis, W., Degorska, A., Santos, S. M. D., Eleftheriadis, K., Fetfatzis, P., Favez, O., Flentje, H.,
872 Gini, M. I., Gregorič, A., Gysel-Beer, M., Hallar, G. A., Hand, J., Hoffer, A., Hueglin, C., Hooda, R. K.,
873 Hyvärinen, A., Kalapov, I., Kalivitis, N., Kasper-Giebl, A., Kim, J. E., Kouvarakis, G., Kranjc, I.,
874 Krejci, R., Kulmala, M., Labuschagne, C., Lee, H.-J., Lihavainen, H., Lin, N.-H., Löschau, G., Luoma,
875 K., Marinoni, A., Meinhardt, F., Merkel, M., Metzger, J.-M., Mihalopoulos, N., Nguyen, N. A.,
876 Ondracek, J., Peréz, N., Perrone, M. R., Petit, J.-E., Picard, D., Pichon, J.-M., Pont, V., Prats, N., Prenni,
877 A., Reisen, F., Romano, S., Sellegri, K., Sharma, S., Schauer, G., Sheridan, P., Sherman, J. P., Schütze,
878 M., Schwerin, A., Sohmer, R., Sorribas, M., Steinbacher, M., Sun, J., Titos, G., Tokzko, B., et al.: A
879 global analysis of climate-relevant aerosol properties retrieved from the network of GAW near-surface
880 observatories, Atmospheric Meas. Tech. Discuss., 1–70, doi:https://doi.org/10.5194/amt-2019-499,
881 2020.

882 Law, K. S. and Stohl, A.: Arctic Air Pollution: Origins and Impacts, Science, 315(5818), 1537–1540,
883 doi:10.1126/science.1137695, 2007.

884 Lim, S., Fain, X., Zanatta, M., Cozic, J., Jaffrezo, J. L., Ginot, P. and Laj, P.: Refractory black carbon
885 mass concentrations in snow and ice : method evaluation and inter-comparison with elemental carbon
886 measurement, Atmospheric Meas. Tech., 7(10), 3307–3324, doi:10.5194/amt-7-3307-2014, 2014.

887 Liu, J., Fan, S., Horowitz, L. W. and Levy, H.: Evaluation of factors controlling long-range transport of
888 black carbon to the Arctic, J. Geophys. Res. Atmospheres, 116(D4), doi:10.1029/2010JD015145, 2011.

https://doi.org/10.5194/acp-2020-574
Preprint. Discussion started: 8 July 2020

Atmospheric Chemistry and Physics Discussions

Lupi, A., Busetto, M., Becagli, S., Giardi, F., Lanconelli, C., Mazzola, M., Udisti, R., Hansson, H.-C., Henning, T., Petkov, B., Ström, J., Krejci, R., Tunved, P., Viola, A. P. and Vitale, V.: Multi-seasonal ultrafine aerosol particle number concentration measurements at the Gruvebadet observatory, Ny-Ålesund, Svalbard Islands, Rendiconti Lincei, 27(1), 59–71, doi:10.1007/s12210-016-0532-8, 2016.

Maturilli, M., Herber, A. and König-Langlo, G.: Climatology and Time Series of Surface Meteorology in Ny¬Ålesund, Svalbard, Earth Syst. Sci. Data, 5, 155–163, doi:Maturilli, M. ORCID: https://orcid.org/0000-0001-6818-7383 <https://orcid.org/0000-0001-6818-7383>, Herber, A. and König-Langlo, G. (2013) Climatology and Time Series of Surface Meteorology in Ny¬Ålesund, Svalbard , Earth System Science Data, 5 , pp. 155-163 . doi:https://doi.org/10.5194/essd-5-155-2013 <https://doi.org/10.5194/essd-5-155-2013> , hdl:10013/epic.41355, 2013.

Maturilli, M., Herber, A. and König-Langlo, G.: Surface radiation climatology for Ny-Ålesund, Svalbard (78.9° N), basic observations for trend detection, Theor. Appl. Climatol., 120(1), 331–339, doi:10.1007/s00704-014-1173-4, 2015.

Maturilli, M., Hanssen-Bauer, I., Neuber, R., Rex, M. and Edvardsen, K.: The Atmosphere Above Ny-Ålesund: Climate and Global Warming, Ozone and Surface UV Radiation, in The Ecosystem of Kongsfjorden, Svalbard, edited by H. Hop and C. Wiencke, pp. 23–46, Springer International Publishing, Cham., 2019.

Moosmüller, H., Chakrabarty, R. K. and Arnott, W. P.: Aerosol light absorption and its measurement: A review, J. Quant. Spectrosc. Radiat. Transf., 110(11), 844–878, doi:10.1016/j.jqsrt.2009.02.035, 2009.

Mori, T., Goto-Azuma, K., Kondo, Y., Ogawa-Tsukagawa, Y., Miura, K., Hirabayashi, M., Oshima, N., Koike, M., Kupiainen, K., Moteki, N., Ohata, S., Sinha, P. R., Sugiura, K., Aoki, T., Schneebeli, M., Steffen, K., Sato, A., Tsushima, A., Makarov, V., Omiya, S., Sugimoto, A., Takano, S. and Nagatsuka, N.: Black Carbon and Inorganic Aerosols in Arctic Snowpack, J. Geophys. Res. Atmospheres, 124(23), 13325–13356, doi:10.1029/2019JD030623, 2019.

Moroni, B., Becagli, S., Bolzacchini, E., Busetto, M., Cappelletti, D., Crocchianti, S., Ferrero, L., Frosini, D., Lanconelli, C., Lupi, A., Maturilli, M., Mazzola, M., Perrone, M. G., Sangiorgi, G., Traversi, R., Udisti, R., Viola, A. and Vitale, V.: Vertical Profiles and Chemical Properties of Aerosol Particles upon Ny-Ålesund (Svalbard Islands), Adv. Meteorol., 2015, e292081, doi:https://doi.org/10.1155/2015/292081, 2015.

Moroni, B., Arnalds, O., Dagsson-Waldhauserová, P., Crocchianti, S., Vivani, R. and Cappelletti, D.: Mineralogical and Chemical Records of Icelandic Dust Sources Upon Ny-Ålesund (Svalbard Islands), Front. Earth Sci., 6, doi:10.3389/feart.2018.00187, 2018.

Moteki, N. and Kondo, Y.: Effects of Mixing State on Black Carbon Measurements by Laser-Induced Incandescence, Aerosol Sci. Technol., 41(4), 398–417, doi:10.1080/02786820701199728, 2007.

Moteki, N. and Kondo, Y.: Dependence of Laser-Induced Incandescence on Physical Properties of Black Carbon Aerosols: Measurements and Theoretical Interpretation, Aerosol Sci. Technol., 44(8), 663–675, doi:10.1080/02786826.2010.484450, 2010.

Motos, G., Schmale, J., Corbin, J. C., Modini, R. L., Karlen, N., Bertò, M., Baltensperger, U. and Gysel-Beer, M.: Cloud droplet activation properties and scavenged fraction of black carbon in liquid-phase clouds at the high-alpine research station Jungfraujoch (3580 m a.s.l.), Atmospheric Chem. Phys., 19(6), 3833–3855, doi:https://doi.org/10.5194/acp-19-3833-2019, 2019.

https://doi.org/10.5194/acp-2020-574
Preprint. Discussion started: 8 July 2020

Atmospheric Chemistry and Physics Discussions

930 Osmont, D., Wendl, I. A., Schmidely, L., Sigl, M., Vega, C. P., Isaksson, E. and Schwikowski, M.: An
931 800-year high-resolution black carbon ice core record from Lomonosovfonna, Svalbard, Atmospheric
932 Chem. Phys., 18(17), 12777–12795, doi:https://doi.org/10.5194/acp-18-12777-2018, 2018.

933 Pedersen, C. A., Gallet, J.-C., Ström, J., Gerland, S., Hudson, S. R., Forsström, S., Isaksson, E. and
934 Berntsen, T. K.: In situ observations of black carbon in snow and the corresponding spectral surface
935 albedo reduction, J. Geophys. Res. Atmospheres, 120(4), 1476–1489, 2015.

936 Petroselli, C., Crocchianti, S., Moroni, B., Castellini, S., Selvaggi, R., Nava, S., Calzolai, G., Lucarelli, F.
937 and Cappelletti, D.: Disentangling the major source areas for an intense aerosol advection in the Central
938 Mediterranean on the basis of Potential Source Contribution Function modeling of chemical and size
939 distribution measurements, Atmospheric Res., 204, 67–77, doi:10.1016/j.atmosres.2018.01.011, 2018.

940 Petzold, A., Ogren, J. A., Fiebig, M., Laj, P., Li, S.-M., Baltensperger, U., Holzer-Popp, T., Kinne, S.,
941 Pappalardo, G., Sugimoto, N., Wehrli, C., Wiedensohler, A. and Zhang, X.-Y.: Recommendations for
942 reporting "black carbon" measurements, Atmospheric Chem. Phys., 13(16), 8365–8379,
943 doi:https://doi.org/10.5194/acp-13-8365-2013, 2013.

944 Programme (AMAP), A. M. and A.: ARCTIC MONITORING AND ASSESSMENT PROGRAMME
945 (AMAP): Work Plan 2015–2017., Working Paper, Arctic Monitoring and Assessment Programme
946 (AMAP). [online] Available from: https://oaarchive.arctic-council.org/handle/11374/1443 (Accessed 6
947 May 2020), 2015.

948 Ramanathan, V. and Carmichael, G.: Global and regional climate changes due to black carbon, Nat.
949 Geosci., 1(4), 221–227, doi:10.1038/ngeo156, 2008.

950 Ruppel, M. M., Soares, J., Gallet, J.-C., Isaksson, E., Martma, T., Svensson, J., Kohler, J., Pedersen, C.
951 A., Manninen, S., Korhola, A. and Ström, J.: Do contemporary (1980–2015) emissions determine the
952 elemental carbon deposition trend at Holtedahlfonna glacier, Svalbard?, Atmospheric Chem. Phys.,
953 17(20), 12779–12795, doi:https://doi.org/10.5194/acp-17-12779-2017, 2017.

954 Scalabrin, E., Zangrando, R., Barbaro, E., Kehrwald, N. M., Gabrieli, J., Barbante, C. and Gambaro, A.:
955 Amino acids in Arctic aerosols, Atmospheric Chem. Phys., 12(21), 10453–10463,
956 doi:https://doi.org/10.5194/acp-12-10453-2012, 2012.

957 Schmale, J., Arnold, S. R., Law, K. S., Thorp, T., Anenberg, S., Simpson, W. R., Mao, J. and Pratt, K. A.:
958 Local Arctic Air Pollution: A Neglected but Serious Problem, Earths Future, 6(10), 1385–1412,
959 doi:10.1029/2018EF000952, 2018.

960 Schwarz, J. P., Gao, R. S., Perring, A. E., Spackman, J. R. and Fahey, D. W.: Black carbon aerosol size in
961 snow, Sci. Rep., 3(1), 1–5, doi:10.1038/srep01356, 2013.

962 Screen, J. A. and Simmonds, I.: The central role of diminishing sea ice in recent Arctic temperature
963 amplification, Nature, 464(7293), 1334–1337, doi:10.1038/nature09051, 2010.

964 Segura, S., Estellés, V., Titos Vela, G., Lyamani, H., Utrilla Navarro, P., Zotter, P., Prévot, A. S. H.,
965 Močnik, G., Alados-Arboledas, L. and Martínez-Lozano, J. A.: Determination and analysis of in situ
966 spectral aerosol optical properties by a multi-instrumental approach, , doi:10.5194/amt-7-2373-2014,
967 2014.

https://doi.org/10.5194/acp-2020-574
Preprint. Discussion started: 8 July 2020

968 Serreze, M. C. and Barry, R. G.: Processes and impacts of Arctic amplification: A research synthesis,
969 Glob. Planet. Change, 77(1), 85–96, doi:10.1016/j.gloplacha.2011.03.004, 2011.

970 Sinha, P. R., Kondo, Y., Goto-Azuma, K., Tsukagawa, Y., Fukuda, K., Koike, M., Ohata, S., Moteki, N.,
971 Mori, T., Oshima, N., Førland, E. J., Irwin, M., Gallet, J.-C. and Pedersen, C. A.: Seasonal Progression
972 of the Deposition of Black Carbon by Snowfall at Ny-Ålesund, Spitsbergen: Deposition of Black
973 Carbon in Spitsbergen, J. Geophys. Res. Atmospheres, 123(2), 997–1016, doi:10.1002/2017JD028027,
974 2018.

975 Skiles, S. M. and Painter, T. H.: Toward Understanding Direct Absorption and Grain Size Feedbacks by
976 Dust Radiative Forcing in Snow With Coupled Snow Physical and Radiative Transfer Modeling, Water
977 Resour. Res., 55(8), 7362–7378, doi:10.1029/2018WR024573, 2019.

978 Skiles, S. M., Flanner, M., Cook, J. M., Dumont, M. and Painter, T. H.: Radiative forcing by light-
979 absorbing particles in snow, Nat. Clim. Change, 8(11), 964–971, doi:10.1038/s41558-018-0296-5, 2018.

980 Spolaor, A., Angot, H., Roman, M., Dommergue, A., Scarchilli, C., Vardè, M., Del Guasta, M., Pedeli,
981 X., Varin, C., Sprovieri, F., Magand, O., Legrand, M., Barbante, C. and Cairns, W. R. L.: Feedback
982 mechanisms between snow and atmospheric mercury: Results and observations from field campaigns on
983 the Antarctic plateau, Chemosphere, 197, 306–317, doi:10.1016/j.chemosphere.2017.12.180, 2018.

984 Spolaor, A., Barbaro, E., Cappelletti, D., Turetta, C., Mazzola, M., Giardi, F., Björkman, M. P.,
985 Lucchetta, F., Dallo, F., Pfaffhuber, K. A., Angot, H., Dommergue, A., Maturilli, M., Saiz-Lopez, A.,
986 Barbante, C. and Cairns, W. R. L.: Diurnal cycle of iodine, bromine, and mercury concentrations in
987 Svalbard surface snow, Atmospheric Chem. Phys., 19(20), 13325–13339,
988 doi:https://doi.org/10.5194/acp-19-13325-2019, 2019.

989 Stein, A. F., Draxler, R. R., Rolph, G. D., Stunder, B. J. B., Cohen, M. D. and Ngan, F.: NOAA's
990 HYSPLIT Atmospheric Transport and Dispersion Modeling System, Bull. Am. Meteorol. Soc., 96(12),
991 2059–2077, doi:10.1175/BAMS-D-14-00110.1, 2015.

992 Stephens, M., Turner, N. and Sandberg, J.: Particle identification by laser-induced incandescence in a
993 solid-state laser cavity, Appl. Opt., 42(19), 3726–3736, doi:10.1364/AO.42.003726, 2003.

994 Tunved, P., Ström, J. and Krejci, R.: Arctic aerosol life cycle: linking aerosol size distributions observed
995 between 2000 and 2010 with air mass transport and precipitation at Zeppelin station, Ny-Ålesund,
996 Svalbard, Atmospheric Chem. Phys., 13(7), 3643–3660, doi:https://doi.org/10.5194/acp-13-3643-2013,
997 2013.

998 Weingartner, E., Saathoff, H., Schnaiter, M., Streit, N., Bitnar, B. and Baltensperger, U.: Absorption of
999 light by soot particles: determination of the absorption coefficient by means of aethalometers, J. Aerosol
1000 Sci., 34(10), 1445–1463, doi:10.1016/S0021-8502(03)00359-8, 2003.

1001 Wendl, I. A., Menking, J. A., Färber, R., Gysel, M., Kaspari, S. D., Laborde, M. J. G. and Schwikowski,
1002 M.: Optimized method for black carbon analysis in ice and snow using the Single Particle Soot
1003 Photometer, Atmospheric Meas. Tech., 7, 2667–2681, doi:10.5194/amt-7-2667-2014, 2014.

1004 Yasunari, T. J., Tan, Q., Lau, K.-M., Bonasoni, P., Marinoni, A., Laj, P., Ménégoz, M., Takemura, T. and
1005 Chin, M.: Estimated range of black carbon dry deposition and the related snow albedo reduction over
1006 Himalayan glaciers during dry pre-monsoon periods, Atmos. Environ., 78, 259–267,
1007 doi:10.1016/j.atmosenv.2012.03.031, 2013.

https://doi.org/10.5194/acp-2020-574
Preprint. Discussion started: 8 July 2020

Atmospheric Chemistry and Physics Discussions

1008 Zanatta, M., Gysel, M., Bukowiecki, N., Müller, T., Weingartner, E., Areskoug, H., Fiebig, M., Yttri, K.
1009 E., Mihalopoulos, N., Kouvarakis, G., Beddows, D., Harrison, R. M., Cavalli, F., Putaud, J. P., Spindler,
1010 G., Wiedensohler, A., Alastuey, A., Pandolfi, M., Sellegri, K., Swietlicki, E., Jaffrezo, J. L.,
1011 Baltensperger, U. and Laj, P.: A European aerosol phenomenology-5: Climatology of black carbon
1012 optical properties at 9 regional background sites across Europe, Atmos. Environ., 145, 346–364,
1013 doi:10.1016/j.atmosenv.2016.09.035, 2016.

1014 Zanatta, M., Laj, P., Gysel, M., Baltensperger, U., Vratolis, S., Eleftheriadis, K., Kondo, Y., Dubuisson,
1015 P., Winiarek, V., Kazadzis, S., Tunved, P. and Jacobi, H.-W.: Effects of mixing state on optical and
1016 radiative properties of black carbon in the European Arctic, Atmospheric Chem. Phys., 18(19), 14037–
1017 14057, doi:https://doi.org/10.5194/acp-18-14037-2018, 2018.

1018 Zangrando, R., Barbaro, E., Zennaro, P., Rossi, S., Kehrwald, N. M., Gabrieli, J., Barbante, C. and
1019 Gambaro, A.: Molecular Markers of Biomass Burning in Arctic Aerosols, Environ. Sci. Technol.,
1020 47(15), 8565–8574, doi:10.1021/es400125r, 2013.

1021